

Numerical Analysis of a Coupled 3D-1D Transport Problem

Alyssa M. Taylor-LaPole^{1*}, Uzochi Gideon¹, Beatrice Riviere¹,
Duygu Vargun¹

¹Department of Computational Applied Mathematics & Operations
Research, Rice University, 6100 Main Street, Houston, 77005, TX, USA.

*Corresponding author(s). E-mail(s): alyssa.lapole@rice.edu;
Contributing authors: uzochi.gideon@rice.edu; riviere@rice.edu;
duygu.vargun@rice.edu;

Abstract

A finite element solution coupled with an interior penalty discontinuous Galerkin solution are defined for the approximation of the coupled 3D-1D solute transport problem. Under sufficient regularity for the weak solutions, optimal error bounds are derived for the 3D concentration and 1D concentration, that are optimal with respect to the time step size and the mesh sizes. Numerical results verify the theoretical results.

Keywords: finite element method, interior penalty discontinuous Galerkin method, well-posedness, error bounds

1 Introduction

Coupled 3D–1D partial differential equations are primarily used to model multi-scale problems in which thin, lower-dimensional structures are embedded within a three-dimensional bulk domain. These models are applied across various scientific and engineering disciplines, ranging from biomedical and physiological sciences [1–4] to geosciences and material sciences [5–9], to address problems characterized by significant disparities in the scales of the domains that constitute the model. Mixed dimensional models avoid the prohibitively high cost of creating a 3D mesh fine enough to resolve the tiny radius of a capillary or well within a large volume, by reducing thin

3D inclusions to 1D manifolds via topological model reduction techniques proposed [10, 11].

In this work, we formulate and analyze a numerical method to solve the coupled 3D-1D time-dependent convection diffusion equations, introduced in [12]. Solute exchange between the 1D and 3D domains is made possible through a flux that is proportional to a permeability function and the difference between the 1D concentration and the lateral average of the 3D concentration. Our scheme combines the backward Euler method in time with the finite element method and with the interior penalty discontinuous Galerkin method in space. Optimal error bounds are derived for the concentration of the solute. Our analysis is valid in the general case where the permeability of the inclusion wall is a non negative function along the 1D domain; this allows for parts of the wall of the blood vessel (or wall of the inclusion) to be impermeable. To our knowledge, our work is the first error analysis of the 3D-1D transport problems.

The numerical analysis of coupled 3D-1D flows is introduced in [11] where the elliptic problem is discretized by the finite element method. Convergence is obtained by deriving a priori error estimates. The authors derive the 3D-1D mixed dimensional model from the fully 3D-3D model and they show that the 3D-1D model has a modeling error that depends on the radius of the tubular inclusion. The coupled 3D-1D elliptic problem is discretized by the interior penalty discontinuous Galerkin method in [13]. Because of the coupling term involving the 1D centerline, the 3D solution exhibits low regularity and consistency of the DG scheme does not hold. The case of numerical discretization of the time-dependent coupled 3D-1D problems has not been studied in the literature. As mentioned above, the work [12] contains the derivation of the 3D-1D transport problem by starting from the 3D-3D models of solute transport and by applying a similar topological reduction to the one in [11]. The authors also show that the modeling error decreases with the inclusion diameter.

An outline of the paper is as follows. We first introduce the model problem and the scheme in Section 2 and Section 3. Existence, uniqueness and stability bounds are obtained in Section 4. Convergence is proved by deriving error bounds in the following section. Numerical results are given in Section 6 and conclusions follow.

2 Model problem

Let $\Omega \subset \mathbb{R}^3$ be a bounded Lipschitz domain and let Λ be \mathcal{C}^2 curve entirely contained in Ω . We parametrize Λ by the function $\lambda(s)$ with $s \in [0, L]$. We assume λ to be the centerline of a generalized cylinder Σ_Λ with boundary Γ . Let γ be the permeability of the boundary. At each point s on Λ , the cross-section is denoted by $\mathcal{D}(s)$ with area $|\mathcal{D}(s)|$ and circumference $|\partial\mathcal{D}(s)|$.

We model the transport of a solute by defining c and \hat{c} the concentrations of the solute in Ω and Λ respectively over the time interval $[0, T]$. The mass balance equations are:

$$\frac{\partial c}{\partial t} - \nabla \cdot (\kappa \nabla c) + \nabla \cdot (\mathbf{U}c) + \gamma(\bar{c} - \hat{c})\delta_\Lambda = f, \text{ in } \Omega \times (0, T), \quad (1)$$

$$|\mathcal{D}(s)|\frac{\partial\hat{c}}{\partial t} - \frac{\partial}{\partial s}\left(|\mathcal{D}(s)|\hat{\kappa}\frac{\partial\hat{c}}{\partial s}\right) + \frac{\partial}{\partial s}\left(|\mathcal{D}(s)|\hat{U}\hat{c}\right) + |\partial\mathcal{D}(s)|\gamma(\hat{c} - \bar{c}) = \hat{f}, \quad \text{in } \Lambda \times (0, T). \quad (2)$$

The interaction between the 1D curve and the 3D domain is done with the term $\gamma(\bar{c} - \hat{c})\delta_\Lambda$, where δ_Λ is the Dirac function on Λ . It is to be understood in the weak sense as follows: for any function $v \in H^1(\Omega)$:

$$\int_\Omega \gamma(\bar{c} - \hat{c})\delta_\Lambda v = \int_\Lambda |\partial\mathcal{D}(s)|(\bar{c} - \hat{c})\bar{v}.$$

The functions \bar{c} and \bar{v} denote the lateral average of c and v respectively. For any $0 \leq s \leq L$ and any function $w \in L^1(\partial\mathcal{D}(s))$, we define

$$\bar{w}(s) = \frac{1}{|\partial\mathcal{D}(s)|} \int_{\partial\mathcal{D}(s)} w.$$

In the model above, κ (resp. $\hat{\kappa}$) denote the diffusion coefficient in Ω (resp. Λ), f (resp. \hat{f}) denote the source/sink function in Ω (resp. Λ), and \mathbf{U} (resp. \hat{U}) denote the velocity field in Ω (resp. Λ).

The initial conditions are:

$$c(\cdot, 0) = c^0(\cdot), \quad \text{in } \Omega, \quad \hat{c}(\cdot, 0) = \hat{c}^0(\cdot), \quad \text{in } \Lambda. \quad (3)$$

We impose zero Dirichlet boundary conditions on the 3D domain

$$c = 0 \quad \text{on } \partial\Omega \times (0, T), \quad (4)$$

and we impose inflow and outflow boundary conditions at the inlet ($s = 0$) and outlet ($s = L$) of Λ . At the inlet, c^{in} denotes a prescribed concentration.

$$|\mathcal{D}|\hat{\kappa}\frac{\partial\hat{c}}{\partial s} - |\mathcal{D}|\hat{U}\hat{c} = -|\mathcal{D}|\hat{U}c^{\text{in}}, \quad \text{at } s = 0, \quad (5)$$

$$|\mathcal{D}|\hat{\kappa}\frac{\partial\hat{c}}{\partial s} = 0, \quad \text{at } s = L. \quad (6)$$

The following assumptions are made on the data.

- (i) The generalized cylinder does not collapse: there are positive constants d_0 and d_1 such that

$$\forall 0 \leq s \leq L, \quad d_0 \leq |\mathcal{D}(s)| \leq d_1, \quad d_0 \leq |\partial\mathcal{D}(s)| \leq d_1. \quad (7)$$

The function $s \mapsto |\mathcal{D}(s)|$ is continuous and piecewise differentiable with non-negative derivative. If Σ_Λ is a cylinder with constant radius, these conditions are trivially satisfied.

- (ii) The functions $\kappa, \hat{\kappa}$ are L^∞ functions, bounded above and below by positive constants. The function $\gamma \in L^\infty(\Gamma)$ is non-negative and bounded.

$$0 < k_0 \leq \kappa(x) \leq k_1, \quad 0 < \hat{k}_0 \leq \hat{\kappa}(s) \leq \hat{k}_1, \quad 0 \leq \gamma \leq \gamma_1.$$

- (iii) The velocities are independent of time. In Λ , the velocity $\hat{U} > 0$ is a positive constant. In Ω , we make some assumptions on the advection field \mathbf{U} , that depend on the divergence of \mathbf{U} . For the analysis below, we differentiate the two cases by introducing a parameter $\eta_{\mathbf{U}} = 0, 1$.

$$\text{Case 1: } \nabla \cdot \mathbf{U} = 0, \quad \eta_{\mathbf{U}} = 0, \quad (8)$$

$$\text{Case 2: } \|\mathbf{U}\|_{L^\infty(\Omega)} \leq \frac{k_0}{2C_0}, \quad \eta_{\mathbf{U}} = 1. \quad (9)$$

The constant C_0 is the Poincaré's constant:

$$\forall v \in H_0^1(\Omega), \quad \|v\|_{L^2(\Omega)} \leq C_0 \|\nabla v\|_{L^2(\Omega)}. \quad (10)$$

- (iv) The source/sink functions and prescribed concentration are continuous in time: $f \in \mathcal{C}(0, T; L^2(\Omega))$, $\hat{f} \in \mathcal{C}(0, T; L^2(\Lambda))$ and $c^{\text{in}} \in \mathcal{C}(0, T)$.
- (v) The initial conditions satisfy: $c^0 \in H^1(\Omega)$ and $\hat{c}^0 \in L^2(\Lambda)$.

A weak solution (c, \hat{c}) is defined such that (c, \hat{c}) satisfies (3), $c \in L^2(0, T; H_0^1(\Omega))$, $\hat{c} \in L^2(0, T; H^1(\Lambda))$ with $\partial_t c \in L^2(0, T; L^2(\Omega))$, $\partial_t \hat{c} \in L^2(0, T; L^2(\Lambda))$ and such that for all $v \in H_0^1(\Omega)$ and $\hat{v} \in H^1(\Lambda)$:

$$\begin{aligned} \int_{\Omega} \frac{\partial c}{\partial t} v + \int_{\Omega} \kappa \nabla c \cdot \nabla v - \int_{\Omega} \mathbf{U} c \cdot \nabla v + \int_{\Lambda} \gamma |\partial \mathcal{D}| (\bar{c} - \hat{c}) \bar{v} &= \int_{\Omega} f v, \\ \int_{\Lambda} |\mathcal{D}| \frac{\partial \hat{c}}{\partial t} \hat{v} + \int_{\Lambda} |\mathcal{D}| \hat{\kappa} \frac{\partial \hat{c}}{\partial s} \frac{\partial \hat{v}}{\partial s} - \int_{\Lambda} |\mathcal{D}| \hat{U} \hat{c} \frac{\partial \hat{v}}{\partial s} + \int_{\Lambda} \gamma |\partial \mathcal{D}| (\hat{c} - \bar{c}) \hat{v} \\ + |\mathcal{D}(L)| \hat{U} \hat{c}(L) \hat{v}(L) &= |\mathcal{D}(0)| \hat{U} c^{\text{in}} \hat{v}(0) + \int_{\Lambda} \hat{f} \hat{v}. \end{aligned}$$

The proof of existence and uniqueness of a weak solution follows a similar argument to the one in [12] (Proposition 4.2).

3 Numerical scheme

The proposed scheme employs the finite element method to solve (1) and the interior penalty discontinuous Galerkin (IPDG) method to solve (2). The time-stepping method is the backward Euler method. The scheme is defined in this section and its derivation is given in Appendix A.

Let $\tau > 0$ denote the time step value and let $t^n = n\tau$ denote the discrete time value for any $n \geq 0$. The domain Ω is partitioned into tetrahedra elements $K \in \mathcal{T}_{\Omega}^h$. The mesh size is defined by $h_{\Omega} = \max_{K \in \mathcal{T}_{\Omega}^h} \text{diam}(K)$. Let V_h^{Ω} be the finite dimensional space

of continuous piecewise polynomials of degree $k_1 \geq 1$ that vanish on the boundary:

$$V_h^\Omega = \{v_h \in H_0^1(\Omega), v_h \in \mathbb{P}_{k_1}(K) \forall K \in \mathcal{T}_\Omega^h\}.$$

Using the parametrization λ , we partition the curve Λ by defining a partition $0 = s_0 < s_1 < \dots < s_N = L$ denoted by \mathcal{T}_Λ^h , with mesh size h_Λ . Let $H^1(\mathcal{T}_\Lambda^h)$ be the space of broken H^1 functions on Ω and V_h^Λ be the finite dimensional space of discontinuous piecewise polynomials of degree k_2 :

$$V_h^\Lambda = \{\hat{v}_h \in L^2(\Lambda), \hat{v}_h \in \mathbb{P}_{k_2}((s_{i-1}, s_i)) \forall i = 1, \dots, N\}.$$

The jump and average operators are defined across interior nodes s_i for $1 \leq i \leq N-1$ as, for any function $\hat{v} \in H^1(\mathcal{T}_\Lambda^h)$:

$$\begin{aligned} \hat{v}(s_i^-) &= \lim_{\epsilon \rightarrow 0, \epsilon > 0} \hat{v}(s_i - \epsilon), \quad \hat{v}(s_i^+) = \lim_{\epsilon \rightarrow 0, \epsilon > 0} \hat{v}(s_i + \epsilon), \\ [\hat{v}]_{s_i} &= \hat{v}(s_i^-) - \hat{v}(s_i^+), \quad \{\hat{v}\}_{s_i} = \frac{1}{2} (\hat{v}(s_i^-) + \hat{v}(s_i^+)). \end{aligned}$$

Let $\sigma > 0$ denote the penalty parameter used in the IPDG scheme. We define a semi-norm for the space V_h^Λ :

$$|\hat{v}_h|_{\text{DG}} = \left(\sum_{i=1}^N \left\| \frac{\partial \hat{v}_h}{\partial s} \right\|_{L^2((s_{i-1}, s_i])}^2 + \frac{\sigma}{h_\Lambda} \sum_{i=1}^{N-1} [\hat{v}_h]_{s_i}^2 \right)^{1/2}.$$

We now present the scheme. For all $n \geq 1$, given $(c_h^{n-1}, \hat{c}_h^{n-1}) \in V_h^\Omega \times V_h^\Lambda$, find $(c_h^n, \hat{c}_h^n) \in V_h^\Omega \times V_h^\Lambda$ such that:

$$\begin{aligned} \frac{1}{\tau} \int_\Omega (c_h^n - c_h^{n-1}) v_h + \int_\Omega \kappa \nabla c_h^n \cdot \nabla v_h - \int_\Omega \mathbf{U} c_h^n \cdot \nabla v_h \\ + \int_\Lambda \gamma |\partial \mathcal{D}| (\bar{c}_h^n - \hat{c}_h^n) \bar{v}_h = \int_\Omega f(\cdot, t^n) v_h, \quad \forall v_h \in V_h^\Omega, \end{aligned} \quad (11)$$

$$\begin{aligned} \frac{1}{\tau} \int_\Lambda |\mathcal{D}| (\hat{c}_h^n - \hat{c}_h^{n-1}) \hat{v}_h + a_\Lambda(\hat{c}_h^n, \hat{v}_h) + b_\Lambda(\hat{c}_h^n, \hat{v}_h) + \int_\Lambda \gamma |\partial \mathcal{D}| (\hat{c}_h^n - \bar{c}_h^n) \hat{v}_h \\ = \int_\Lambda \hat{f}(\cdot, t^n) \hat{v}_h + |\mathcal{D}(0)| \hat{U} c^{\text{in}}(t^n) \hat{v}_h(0), \quad \forall \hat{v}_h \in V_h^\Lambda, \end{aligned} \quad (12)$$

where $a_\Lambda(\cdot, \cdot)$ and $b_\Lambda(\cdot, \cdot)$ are defined as follows for any $\hat{\xi}, \hat{v}$:

$$\begin{aligned} a_\Lambda(\hat{\xi}, \hat{v}) &= \sum_{i=1}^N \int_{s_{i-1}}^{s_i} |\mathcal{D}| \hat{\kappa} \frac{\partial \hat{\xi}}{\partial s} \frac{\partial \hat{v}}{\partial s} - \sum_{i=1}^{N-1} \{ |\mathcal{D}| \hat{\kappa} \frac{\partial \hat{\xi}}{\partial s} \}_{s_i} [\hat{v}]_{s_i} \\ &\quad - \epsilon \sum_{i=1}^{N-1} \{ |\mathcal{D}| \hat{\kappa} \frac{\partial \hat{v}}{\partial s} \}_{s_i} [\hat{\xi}]_{s_i} + \sum_{i=1}^{N-1} \frac{\sigma}{h_\Lambda} [\hat{\xi}]_{s_i} [\hat{v}]_{s_i}, \end{aligned}$$

$$b_\Lambda(\hat{\xi}, \hat{v}) = - \sum_{i=1}^N \int_{s_{i-1}}^{s_i} |\mathcal{D}| \hat{U} \hat{\xi} \frac{\partial \hat{v}}{\partial s} + \sum_{i=1}^{N-1} |\mathcal{D}(s_i)| \hat{U} \hat{\xi}(s_i^-) [\hat{v}]_{s_i} + |\mathcal{D}(L)| \hat{U} \hat{\xi}(L) \hat{v}(L).$$

We remark that a_Λ is the standard IPDG discretization of the diffusion operator and b_Λ is a slightly modified discretization of the advection operator, that takes into account the weight $|\mathcal{D}|$. The parameter ϵ in a_Λ takes the value -1 , 0 or $+1$ to yield the classical variations of the IPDG method.

To start the scheme, we choose

$$c_h^0 = \Pi c^0, \quad \hat{c}_h^0 = \pi \hat{c}^0,$$

where Πc^0 is the Scott-Zhang interpolant of c^0 [14] and $\pi \hat{c}^0$ is the L^2 projection of \hat{c}^0 onto V_h^Λ .

Throughout the paper, M will denote a generic positive constant that is independent of h and τ and takes different values at different places.

4 Well-posedness

Before we state and prove existence and uniqueness of the discrete solution, we present some important properties of the bilinear forms a_Λ and b_Λ . Throughout the paper, we assume that if $\epsilon = 1, 0$ the penalty parameter σ is large enough, and if $\epsilon = -1$ the penalty parameter is chosen $\sigma = 1$. Under this assumption, coercivity of a_Λ holds (see proof in Appendix B): there is a constant $C_a > 0$ such that

$$\forall \hat{v} \in V_h^\Lambda, \quad C_a |\hat{v}|_{\text{DG}}^2 \leq a_\Lambda(\hat{v}, \hat{v}). \quad (13)$$

The proof of the positivity of b_Λ is provided in Appendix C.

$$\forall \hat{v} \in V_h^\Lambda, \quad \frac{1}{2} \sum_{i=1}^{N-1} |\mathcal{D}(s_i)| \hat{U} [\hat{v}]_{s_i}^2 + \frac{1}{2} |\mathcal{D}(0)| \hat{U} (\hat{v}(0))^2 + \frac{1}{2} |\mathcal{D}(L)| \hat{U} (\hat{v}(L))^2 \leq b_\Lambda(\hat{v}, \hat{v}). \quad (14)$$

Lemma 1 *For each $n \geq 1$, there exists a unique solution $(c_h^n, \hat{c}_h^n) \in V_h^\Omega \times V_h^\Lambda$ satisfying (11)-(12). In addition, if $\tau \leq 1/2$, there is a constant $M > 0$ independent of h and τ such that*

$$\begin{aligned} \forall m \geq 1, \quad & \|c_h^m\|_{L^2(\Omega)}^2 + d_0 \|\hat{c}_h^m\|_{L^2(\Lambda)}^2 + \tau k_0 \sum_{n=1}^m \|\nabla c_h^n\|_{L^2(\Omega)}^2 + \tau C_a \sum_{n=1}^m |\hat{c}_h^n|_{\text{DG}}^2 \\ & \leq M\tau \sum_{n=1}^m \|f(\cdot, t^n)\|_{L^2(\Omega)}^2 + M\tau \sum_{n=1}^m \|\hat{f}(\cdot, t^n)\|_{L^2(\Lambda)}^2 \\ & \quad + M|\mathcal{D}(0)| \hat{U} \tau \sum_{n=1}^m (c^{\text{in}}(t^n))^2 + C \|c^0\|_{H^s(\Omega)}^2 + M \|\hat{c}^0\|_{H^r(\Lambda)}^2. \end{aligned} \quad (15)$$

Proof Assume that $n \geq 1$. Since the problem is linear and finite-dimensional, it suffices to show uniqueness of the solutions. Assume that $(w, \hat{w}) = (c_h^{n,1} - c_h^{n,2}, \hat{c}_h^{n,1} - \hat{c}_h^{n,2})$, is the pair of differences between two solution pairs. It suffices to show $(w, \hat{w}) = (0, 0)$. By linearity, we have for all $(v_h, \hat{v}_h) \in V_h^\Omega \times V_h^\Lambda$

$$\begin{aligned} \frac{1}{\tau} \int_{\Omega} w v_h + \int_{\Omega} \kappa \nabla w \cdot \nabla v_h - \int_{\Omega} \mathbf{U} w \cdot \nabla v_h + \int_{\Lambda} \gamma |\partial \mathcal{D}| (\bar{w} - \hat{w}) \bar{v}_h &= 0, \\ \frac{1}{\tau} \int_{\Lambda} |\mathcal{D}| \hat{w} \hat{v}_h + a_{\Lambda}(\hat{w}, \hat{v}_h) + b_{\Lambda}(\hat{w}, \hat{v}_h) + \int_{\Lambda} \gamma |\partial \mathcal{D}| (\hat{w} - \bar{w}) \hat{v}_h &= 0. \end{aligned}$$

We add the two equations and choose $(v_h, \hat{v}_h) = (w, \hat{w})$. Using the coercivity of a_{Λ} and the positivity of b_{Λ} , we have

$$\begin{aligned} \frac{1}{\tau} \|w\|_{L^2(\Omega)}^2 + \|\kappa^{1/2} \nabla w\|_{L^2(\Omega)}^2 - \int_{\Omega} \mathbf{U} w \cdot \nabla w + \|\gamma^{1/2} |\partial \mathcal{D}|^{1/2} (\bar{w} - \hat{w})\|_{L^2(\Lambda)}^2 \\ + \frac{1}{\tau} \|\mathcal{D}|^{1/2} \hat{w}\|_{L^2(\Lambda)}^2 + C_a |\hat{w}|_{\text{DG}}^2 \leq 0. \end{aligned}$$

In the case where $\nabla \cdot \mathbf{U} = 0$, we have

$$\int_{\Omega} \mathbf{U} w \cdot \nabla w = 0,$$

so the third term above disappears. It is then easy to conclude that $w = \hat{w} = 0$ by using the coercivity of a_{Λ} and the positivity of b_{Λ} . In the case where \mathbf{U} is non-divergence free, we write with Poincaré's inequality

$$\begin{aligned} \int_{\Omega} \mathbf{U} w \cdot \nabla w &\leq \|\mathbf{U}\|_{L^\infty(\Omega)} \|w\|_{L^2(\Omega)} \|\nabla w\|_{L^2(\Omega)} \\ &\leq C_0 \|\mathbf{U}\|_{L^\infty(\Omega)} \|\nabla w\|_{L^2(\Omega)}^2 \end{aligned}$$

Therefore we have

$$(k_0 - C_0 \|\mathbf{U}\|_{L^\infty(\Omega)}) \|\nabla w\|_{L^2(\Omega)}^2 \leq \|\kappa^{1/2} \nabla w\|_{L^2(\Omega)}^2 - \int_{\Omega} \mathbf{U} w \cdot \nabla w.$$

Since \mathbf{U} satisfies (9), it is then easy to conclude that $w = \hat{w} = 0$. Thus, we have proved uniqueness, which is equivalent to proving existence.

Next, we show the stability bound (15). We choose $(v_h, \hat{v}_h) = (c_h^n, \hat{c}_h^n)$ in (11)-(12). We sum the resulting equations and use coercivity of a_{Λ} and positivity of b_{Λ} to obtain:

$$\begin{aligned} \frac{1}{\tau} \int_{\Omega} (c_h^n - c_h^{n-1}) c_h^n + \frac{1}{\tau} \int_{\Lambda} |\mathcal{D}| (\hat{c}_h^n - \hat{c}_h^{n-1}) \hat{c}_h^n + (k_0 - C_0 \eta_{\mathbf{U}} \|\mathbf{U}\|_{L^\infty(\Omega)}) \|\nabla c_h^n\|_{L^2(\Omega)}^2 \\ + C_a |\hat{c}_h^n|_{\text{DG}}^2 + \|\gamma^{1/2} |\partial \mathcal{D}|^{1/2} (\bar{c}_h^n - \hat{c}_h^n)\|_{L^2(\Lambda)}^2 + \frac{1}{2} |\mathcal{D}(0)| \hat{U} (\hat{c}_h^n(0))^2 \\ \leq \int_{\Omega} f(\cdot, t^n) c_h^n + \int_{\Lambda} \hat{f}(\cdot, t^n) \hat{c}_h^n + |\mathcal{D}(0)| \hat{U} c^{\text{in}}(t^n) \hat{c}_h^n(0). \end{aligned} \quad (16)$$

Next we observe that for the two cases we consider, we have

$$k_0 - C_0 \eta_{\mathbf{U}} \|\mathbf{U}\|_{L^\infty(\Omega)} \geq \frac{k_0}{2}. \quad (17)$$

Using Cauchy-Schwarz's inequality we have

$$\int_{\Omega} f(\cdot, t^n) c_h^n + \int_{\Lambda} \hat{f}(\cdot, t^n) \hat{c}_h^n \leq \frac{1}{2} \|c_h^n\|_{L^2(\Omega)}^2 + \frac{1}{2} \|\hat{c}_h^n\|_{L^2(\Lambda)}^2 + \frac{1}{2} \|f(\cdot, t^n)\|_{L^2(\Omega)}^2 + \frac{1}{2} \|\hat{f}(\cdot, t^n)\|_{L^2(\Lambda)}^2.$$

We also have with Young's inequality:

$$|\mathcal{D}(0)| \hat{U} c^{\text{in}}(t^n) \hat{c}_h^n(0) \leq \frac{1}{4} |\mathcal{D}(0)| \hat{U} (\hat{c}_h^n(0))^2 + |\mathcal{D}(0)| \hat{U} (c^{\text{in}}(t^n))^2.$$

Therefore the bound (16) becomes

$$\begin{aligned} & \frac{1}{2\tau} (\|c_h^n\|_{L^2(\Omega)}^2 - \|c_h^{n-1}\|_{L^2(\Omega)}^2) + \frac{d_0}{2\tau} (\|\hat{c}_h^n\|_{L^2(\Lambda)}^2 - \|\hat{c}_h^{n-1}\|_{L^2(\Lambda)}^2) + \frac{k_0}{2} \|\nabla c_h^n\|_{L^2(\Omega)}^2 \\ & + C_a |c_h^n|_{\text{DG}}^2 + \|\gamma^{1/2} |\partial \mathcal{D}|^{1/2} (\bar{c}_h^n - \hat{c}_h^n)\|_{L^2(\Lambda)}^2 \leq \frac{1}{2} \|c_h^n\|_{L^2(\Omega)}^2 + \frac{1}{2} \|\hat{c}_h^n\|_{L^2(\Lambda)}^2 \\ & + \frac{1}{2} \|f(\cdot, t^n)\|_{L^2(\Omega)}^2 + \frac{1}{2} \|\hat{f}(\cdot, t^n)\|_{L^2(\Lambda)}^2 + |\mathcal{D}(0)| \hat{U}(c^{\text{in}}(t^n))^2. \end{aligned} \quad (18)$$

To conclude, we multiply by 2τ , sum from $n = 1$ to $n = m$, use the stability of the L^2 projection of \hat{c}^0 in the L^2 norm, the approximation bound of the Scott-Zhang interpolant of c^0 and use Gronwall's lemma. \square

5 Error analysis

To handle the coupling term in the analysis below, we will make use of the following result (see Lemma 3.4 in [11]).

Lemma 2 *The following inequality holds*

$$\forall v \in H^1(\Omega), \quad \| |\partial \mathcal{D}|^{1/2} \bar{v} \|_{L^2(\Lambda)} \leq \|v\|_{L^2(\Gamma)} \leq C_1 \|v\|_{H^1(\Omega)},$$

where C_1 is the positive constant of the trace inequality from $L^2(\Gamma)$ to $H^1(\Omega)$.

Now, under sufficient regularity for the weak solution, we state and prove an error bound that is optimal in time and space with respect to the gradient norm.

Theorem 3 *Let (c, \hat{c}) be the weak solution and assume that $c \in L^2(0, T; H^r(\Omega))$, for $1 < r < 3/2$, $\hat{c} \in L^2(0, T; H^2(\Omega))$, $\frac{\partial c}{\partial t} \in L^2(0, T; H^r(\Omega))$ and $\frac{\partial^2 c}{\partial t^2} \in L^2([0, T] \times \Omega)$. Assume τ is small enough, namely $\tau \leq \frac{1}{2}$. There exists a constant $M > 0$ independent of h_Ω, h_Λ and τ such that for all $m \geq 1$*

$$\begin{aligned} & \|c(\cdot, t^m) - c_h^m\|_{L^2(\Omega)}^2 + \|\hat{c}(\cdot, t^m) - c_h^m\|_{L^2(\Lambda)}^2 \\ & + \tau \sum_{n=1}^m \|\nabla c(\cdot, t^n) - \nabla c_h^n\|_{L^2(\Omega)}^2 + \tau \sum_{n=1}^m \|\hat{c}(\cdot, t^n) - \hat{c}_h^n\|_{\text{DG}}^2 \leq M(\tau^2 + h_\Omega^{2r-2} + h_\Lambda^2). \end{aligned} \quad (19)$$

Proof We will first obtain error bounds for the errors between the numerical solutions and optimal approximations of the weak solutions. We introduce the notation:

$$\begin{aligned} \forall n \geq 0, \quad e^n &= c_h^n - \Pi c(t^n), \quad \hat{e}^n = \hat{c}_h^n - \pi \hat{c}(t^n), \\ \forall t \geq 0, \quad \xi(t) &= c(t) - \Pi c(t), \quad \hat{\xi}(t) = \hat{c}(t) - \pi \hat{c}(t), \end{aligned}$$

where for all t , $\Pi c(t) \in H_0^1(\Omega)$ is the Scott-Zhang interpolant of $c(t)$ and $\pi \hat{c}(t)$ is the L^2 projection of $\hat{c}(t)$ on V_h^Λ . These approximations satisfy the following optimal bounds [15]:

$$\|\xi(t)\|_{L^2(\Omega)} \leq M h_\Omega^r \|c(t)\|_{H^r(\Omega)}, \quad \|\partial_t \xi(t)\|_{L^2(\Omega)} \leq M h_\Omega^r \|\partial_t c(t)\|_{H^r(\Omega)}, \quad (20)$$

$$\|\nabla \xi(t)\|_{L^2(\Omega)} \leq M h_\Omega^{r-1} \|c(t)\|_{H^r(\Omega)}, \quad (21)$$

$$\forall 1 \leq i \leq N, \quad \|\hat{\xi}(t)\|_{L^2([s_{i-1}, s_i])} \leq M h_\Lambda^2 \|\hat{c}(t)\|_{H^2(s_{i-1}, s_i)}, \quad (22)$$

$$\forall 1 \leq i \leq N, \|\partial_t \hat{\xi}(t)\|_{L^2([s_{i-1}, s_i])} \leq M h_\Lambda^2 \|\partial_t \hat{c}(t)\|_{H^2([s_{i-1}, s_i])}, \quad (23)$$

$$\forall 1 \leq i \leq N, \left\| \frac{\partial \hat{\xi}(t)}{\partial s} \right\|_{L^2([s_{i-1}, s_i])} + h_\Lambda \left\| \frac{\partial^2 \hat{\xi}(t)}{\partial s^2} \right\|_{L^2([s_{i-1}, s_i])} \leq M h_\Lambda \|\hat{c}(t)\|_{H^2([s_{i-1}, s_i])}. \quad (24)$$

The bounds hold for the time derivatives because $\partial_t \Pi c = \Pi \partial_t c$ and $\partial_t \pi c = \pi \partial_t c$.

With the regularity assumptions on the weak solution, it is easy to see that it satisfies for all $n \geq 1$:

$$\begin{aligned} \int_\Omega \frac{\partial c}{\partial t}(t^n) v_h + \int_\Omega \kappa \nabla c(t^n) \cdot \nabla v_h - \int_\Omega \mathbf{U} c(t^n) \cdot \nabla v_h + \int_\Lambda \gamma |\partial \mathcal{D}| \left(\overline{c(t^n)} - \hat{c}(t^n) \right) \overline{v_h} \\ = \int_\Omega f(\cdot, t^n) v_h, \quad \forall v_h \in V_h^\Omega, \end{aligned}$$

and

$$\begin{aligned} \int_\Lambda |\mathcal{D}| \frac{\partial \hat{c}(t^n)}{\partial t} \hat{v}_h + a_\Lambda(\hat{c}(t^n), \hat{v}_h) + b_\Lambda(\hat{c}(t^n), \hat{v}_h) \\ + \int_\Lambda \gamma |\partial \mathcal{D}| \left(\hat{c}(t^n) - \overline{c(t^n)} \right) \hat{v}_h = |\mathcal{D}(0)| \hat{U} c^{\text{in}}(t^n) \hat{v}_h(0) + \int_\Lambda \hat{f}(\cdot, t^n) \hat{v}_h, \quad \forall \hat{v}_h \in V_h^\Lambda. \end{aligned}$$

Therefore we have the following error equations

$$\begin{aligned} \frac{1}{\tau} \int_\Omega (e^n - e^{n-1}) v_h + \int_\Omega \kappa \nabla e^n \cdot \nabla v_h - \int_\Omega \mathbf{U} e^n \cdot \nabla v_h + \int_\Lambda \gamma |\partial \mathcal{D}| (\overline{e^n} - \hat{e}^n) \overline{v_h} \\ = \int_\Omega \left(\frac{\partial c}{\partial t}(t^n) - \frac{1}{\tau} (\Pi c(t^n) - \Pi c(t^{n-1})) \right) v_h + \int_\Omega \kappa \nabla \xi(t^n) \cdot \nabla v_h - \int_\Omega \mathbf{U} \xi(t^n) \cdot \nabla v_h \\ + \int_\Lambda \gamma |\partial \mathcal{D}| \left(\overline{\xi(t^n)} - \hat{\xi}(t^n) \right) \overline{v_h}, \quad \forall v_h \in V_h^\Omega, \quad (25) \end{aligned}$$

and

$$\begin{aligned} \frac{1}{\tau} \int_\Lambda |\mathcal{D}| (\hat{e}^n - \hat{e}^{n-1}) \hat{v}_h + a_\Lambda(\hat{e}^n, \hat{v}_h) + b_\Lambda(\hat{e}^n, \hat{v}_h) + \int_\Lambda \gamma |\partial \mathcal{D}| (\hat{e}^n - \overline{e^n}) \hat{v}_h \\ = \int_\Lambda |\mathcal{D}| \left(\frac{\partial \hat{c}}{\partial t} - \frac{1}{\tau} (\pi \hat{c}(t^n) - \pi \hat{c}(t^{n-1})) \right) \hat{v}_h + a_\Lambda(\hat{\xi}(t^n), \hat{v}_h) + b_\Lambda(\hat{\xi}(t^n), \hat{v}_h) \\ + \int_\Lambda \gamma |\partial \mathcal{D}| \left(\hat{\xi}(t^n) - \overline{\xi(t^n)} \right) \hat{v}_h, \quad \forall \hat{v}_h \in V_h^\Lambda. \quad (26) \end{aligned}$$

Choosing $v_h = e^n$ in (25) and $v_h = \hat{e}^n$ in (26), summing the two resulting equations, using coercivity of a_Λ , property (17) and the positivity of b_Λ , we have

$$\begin{aligned} \frac{1}{2\tau} \left(\|e^n\|_{L^2(\Omega)}^2 - \|e^{n-1}\|_{L^2(\Omega)}^2 \right) + \frac{1}{2\tau} \left(\|\mathcal{D}\|^{1/2} \hat{e}^n \|_{L^2(\Lambda)}^2 - \|\mathcal{D}\|^{1/2} \hat{e}^{n-1} \|_{L^2(\Lambda)}^2 \right) \\ + \|\gamma^{1/2} |\partial \mathcal{D}|^{1/2} (\overline{e^n} - \hat{e}^n) \|_{L^2(\Lambda)}^2 + \frac{k_0}{2} \|\nabla e^n\|_{L^2(\Omega)}^2 + C_a |\hat{e}^n|_{\text{DG}}^2 \\ + \frac{1}{2} \sum_{i=1}^{N-1} |\mathcal{D}(s_i)| \hat{U} ([\hat{e}^n]_{s_i})^2 + \frac{1}{2} |\mathcal{D}(0)| \hat{U} (\hat{e}^n(0))^2 + \frac{1}{2} |\mathcal{D}(L)| \hat{U} (\hat{e}^n(L))^2 \\ \leq \int_\Omega \left(\frac{dc}{dt}(t^n) - \frac{1}{\tau} (\Pi c(t^n) - \Pi c(t^{n-1})) \right) e^n + \int_\Lambda |\mathcal{D}| \left(\frac{d\hat{c}}{dt} - \frac{1}{\tau} (\pi \hat{c}(t^n) - \pi \hat{c}(t^{n-1})) \right) \hat{e}^n \\ + \int_\Omega \kappa \nabla \xi(t^n) \cdot \nabla e^n - \int_\Omega \mathbf{U} \xi(t^n) \cdot \nabla e^n + a_\Lambda(\hat{\xi}(t^n), \hat{e}^n) + b_\Lambda(\hat{\xi}(t^n), \hat{e}^n) \\ + \int_\Lambda \gamma |\partial \mathcal{D}| \left(\overline{\xi(t^n)} - \hat{\xi}(t^n) \right) (\overline{e^n} - \hat{e}^n) \end{aligned}$$

$$= T_1 + \dots + T_7.$$

We now bound each term T_i . For the first two terms T_1 and T_2 , we will use the well-known equality for any function w of one variable t :

$$\frac{1}{\tau}(w(t^n) - w(t^{n-1})) = w'(t^n) - \frac{1}{\tau} \int_{t^{n-1}}^{t^n} (s - t^{n-1})w''(s)ds.$$

Using Cauchy-Schwarz's inequality, Young's inequality with a positive ϵ_1 parameter, (10) and the approximation bound (20), we have for T_1 :

$$\begin{aligned} T_1 &= \int_{\Omega} \left(\frac{dc}{dt}(t^n) - \frac{1}{\tau}(\Pi c(t^n) - \Pi c(t^{n-1})) \right) e^n \\ &= \int_{\Omega} \left(\frac{dc}{dt}(t^n) - \frac{1}{\tau}(c(t^n) - c(t^{n-1})) \right) e^n + \frac{1}{\tau} \int_{\Omega} (\xi(t^n) - \xi(t^{n-1})) e^n \\ &\leq M\sqrt{\tau} \|e^n\|_{L^2(\Omega)} \left\| \frac{\partial^2 c}{\partial t^2} \right\|_{L^2([t^{n-1}, t^n] \times \Omega)} + \frac{1}{\tau} \int_{\Omega} e^n \left(\int_{t^{n-1}}^{t^n} \frac{\partial \xi}{\partial t} \right) \\ &\leq \epsilon_1 \|\nabla e^n\|_{L^2(\Omega)}^2 + \frac{M}{2\epsilon_1} \tau \left\| \frac{\partial^2 c}{\partial t^2} \right\|_{L^2([t^{n-1}, t^n] \times \Omega)}^2 + M \frac{h_{\Omega}^{2r}}{\epsilon_1 \tau} \left\| \frac{\partial c}{\partial t} \right\|_{L^2(t^{n-1}, t^n; H^r(\Omega))}^2. \end{aligned}$$

The second term is bounded in a similar fashion as the first term, except we do not use Poincaré's inequality. The approximation bound (23) and Young's inequality with parameter $\epsilon_2 > 0$ are used.

$$T_2 \leq \epsilon_2 \|\hat{e}^n\|_{L^2(\Lambda)}^2 + \frac{M}{2\epsilon_2} \tau \left\| \frac{\partial^2 \hat{c}}{\partial t^2} \right\|_{L^2([t^{n-1}, t^n] \times \Lambda)}^2 + M \frac{h_{\Lambda}^4}{2\epsilon_2 \tau} \left\| \frac{\partial \hat{c}}{\partial t} \right\|_{L^2(t^{n-1}, t^n; H^2(\Lambda))}^2.$$

The third term is bounded using Cauchy-Schwarz's and Young's inequalities and the approximation bound (21):

$$\begin{aligned} T_3 &\leq \frac{\epsilon_3}{2} \|\nabla e^n\|_{L^2(\Omega)}^2 + \frac{1}{2\epsilon_3} k_1^2 \|\nabla \xi(t^n)\|_{L^2(\Omega)}^2 \\ &\leq \frac{\epsilon_3}{2} \|\nabla e^n\|_{L^2(\Omega)}^2 + \frac{Mk_1^2}{2\epsilon_3} h_{\Omega}^{2r-2} \|c(t^n)\|_{H^r(\Omega)}^2. \end{aligned}$$

Similarly, with Cauchy-Schwarz's, Young's inequalities and the approximation property (20), we have for the fourth term:

$$\begin{aligned} T_4 &\leq \frac{\epsilon_4}{2} \|\nabla e^n\|_{L^2(\Omega)}^2 + \frac{1}{2\epsilon_4} \|\mathbf{U}\|_{L^\infty(\Omega)}^2 \|\xi(t^n)\|_{L^2(\Omega)}^2 \\ &\leq \frac{\epsilon_4}{2} \|\nabla e^n\|_{L^2(\Omega)}^2 + \frac{M}{2\epsilon_4} \|\mathbf{U}\|_{L^\infty(\Omega)}^2 h_{\Omega}^{2r} \|c(t^n)\|_{H^r(\Omega)}^2. \end{aligned}$$

Using standard DG techniques to bound the terms in the DG bilinear form ([16], see Appendix D):

$$T_5 \leq \frac{\epsilon_5}{2} |e^n|_{\text{DG}}^2 + \frac{1}{2\epsilon_5} M h_{\Lambda}^2 \|\hat{c}(t^n)\|_{H^2(\Lambda)}^2.$$

For the sixth term, we have with (22), (24), a trace inequality, Cauchy-Schwarz's and Young's inequalities:

$$\begin{aligned} T_6 &= - \sum_{i=1}^N \int_{s_{i-1}}^{s_i} |\mathcal{D}| \hat{U} \hat{\xi}(t^n) \frac{\partial \hat{e}^n}{\partial s} + \sum_{i=1}^{N-1} |\mathcal{D}(s_i)| \hat{U} \hat{\xi}(s_i^-, t^n) [\hat{e}^n]_{s_i} \\ &\quad + |\mathcal{D}(L)| \hat{U} \hat{\xi}(L, t^n) (\hat{e}^n(L)) \end{aligned}$$

$$\begin{aligned}
&\leq d_1 \sum_{i=1}^N \hat{U} \left\| \frac{\partial \hat{e}^n}{\partial s} \right\|_{L^2(s_{i-1}, s_i)} \|\hat{\xi}(t^n)\|_{L^2(s_{i-1}, s_i)} + \frac{1}{4} \sum_{i=1}^{N-1} |\mathcal{D}(s_i)| \hat{U} [\hat{e}^n]_{s_i}^2 \\
&\quad + \sum_{i=1}^{N-1} \hat{U} |\mathcal{D}(s_i)| \hat{\xi}(s_i^-, t^n)^2 + \frac{1}{4} |\mathcal{D}(L)| \hat{U} (\hat{e}^n(L))^2 + |\mathcal{D}(L)| \hat{U} \hat{\xi}(L, t^n)^2 \\
&\leq \frac{\epsilon_6}{2} |\hat{e}^n|_{\text{DG}}^2 + \frac{d_1^2}{2\epsilon_6} \hat{U}^2 \sum_{i=1}^N \|\hat{\xi}(t^n)\|_{L^2(s_{i-1}, s_i)}^2 + \frac{1}{4} \sum_{i=1}^{N-1} |\mathcal{D}(s_i)| \hat{U} [\hat{e}^n]_{s_i}^2 \\
&\quad + \sum_{i=1}^{N-1} \hat{U} |\mathcal{D}(s_i)| \hat{\xi}(s_i^-, t^n)^2 + \frac{1}{4} |\mathcal{D}(L)| \hat{U} (\hat{e}^n(L))^2 + |\mathcal{D}(L)| \hat{U} \hat{\xi}(L, t^n)^2 \\
&\leq \frac{\epsilon_6}{2} |\hat{e}^n|_{\text{DG}}^2 + M \frac{d_1^2}{2\epsilon_6} \hat{U}^2 h_\Lambda^4 \|\hat{c}(t^n)\|_{H^2(\Lambda)}^2 + \frac{1}{4} \sum_{i=1}^{N-1} |\mathcal{D}(s_i)| \hat{U} [\hat{e}^n]_{s_i}^2 \\
&\quad + \frac{1}{4} |\mathcal{D}(L)| \hat{U} (\hat{e}^n(L))^2 + M d_1 \hat{U} h_\Lambda^3 \|\hat{c}(t^n)\|_{H^2(\Lambda)}^2.
\end{aligned}$$

For the last term, we first write

$$T_7 \leq \frac{1}{2} \|\gamma^{1/2} |\partial \mathcal{D}|^{1/2} (\bar{e}^n - \hat{e}^n)\|_{L^2(\Lambda)}^2 + \frac{1}{2} \|\gamma^{1/2} |\partial \mathcal{D}|^{1/2} (\bar{\xi}(t^n) - \hat{\xi}(t^n))\|_{L^2(\Lambda)}^2$$

Using triangle inequality, Lemma 2, and approximation results (22), (20) and (21), we obtain:

$$\begin{aligned}
\|\gamma^{1/2} |\partial \mathcal{D}|^{1/2} (\bar{\xi}(t^n) - \hat{\xi}(t^n))\|_{L^2(\Lambda)} &\leq \gamma_1 \|\partial \mathcal{D}^{1/2} \bar{\xi}(t^n)\|_{L^2(\Lambda)} + \gamma_1 \|\partial \mathcal{D}^{1/2} \hat{\xi}(t^n)\|_{L^2(\Lambda)} \\
&\leq \gamma_1 C_1 \|\xi(t^n)\|_{H^1(\Omega)} + \gamma_1 d_1 M h_\Lambda^2 \|\hat{c}(t^n)\|_{H^2(\Lambda)} \\
&\leq \gamma_1 C_1 M h_\Omega^{r-1} \|c(t^n)\|_{H^r(\Omega)} + \gamma_1 d_1 M h_\Lambda^2 \|\hat{c}(t^n)\|_{H^2(\Lambda)}.
\end{aligned}$$

Therefore a bound for T_7 is

$$T_7 \leq \frac{1}{2} \|\gamma^{1/2} |\partial \mathcal{D}|^{1/2} (\bar{e}^n - \hat{e}^n)\|_{L^2(\Lambda)}^2 + M h_\Omega^{2r-2} \|c(t^n)\|_{H^r(\Omega)}^2 + M h_\Lambda^4 \|\hat{c}(t^n)\|_{H^2(\Lambda)}^2.$$

We choose the following values for the parameters ϵ_i :

$$\epsilon_1 = \frac{k_0}{12}, \quad \epsilon_2 = d_0, \quad \epsilon_3 = \epsilon_4 = \frac{k_0}{6}, \quad \epsilon_5 = \epsilon_6 = \frac{C_a}{2},$$

and combine the bounds above to obtain

$$\begin{aligned}
&\frac{1}{2\tau} \left(\|e^n\|_{L^2(\Omega)}^2 - \|e^{n-1}\|_{L^2(\Omega)}^2 \right) + \frac{1}{2\tau} \left(\|\mathcal{D}^{1/2} \hat{e}^n\|_{L^2(\Lambda)}^2 - \|\mathcal{D}^{1/2} \hat{e}^{n-1}\|_{L^2(\Lambda)}^2 \right) \\
&\quad + \frac{1}{2} \|\gamma^{1/2} |\partial \mathcal{D}|^{1/2} (\bar{e}^n - \hat{e}^n)\|_{L^2(\Lambda)}^2 + \frac{k_0}{4} \|\nabla e^n\|_{L^2(\Omega)}^2 + \frac{C_a}{2} |\hat{e}^n|_{\text{DG}}^2 \\
&\quad + \frac{1}{4} \sum_{i=1}^{N-1} |\mathcal{D}(s_i)| \hat{U} ([\hat{e}^n]_{s_i})^2 + \frac{1}{2} |\mathcal{D}(0)| \hat{U} (\hat{e}^n(0))^2 + \frac{1}{4} |\mathcal{D}(L)| \hat{U} (\hat{e}^n(L))^2 \\
&\leq \|\mathcal{D}^{1/2} \hat{e}^n\|_{L^2(\Lambda)}^2 + M\tau \left(\left\| \frac{\partial^2 c}{\partial t^2} \right\|_{L^2([t^{n-1}, t^n] \times \Omega)}^2 + \left\| \frac{\partial^2 \hat{c}}{\partial t^2} \right\|_{L^2([t^{n-1}, t^n] \times \Lambda)}^2 \right) \\
&\quad + M \frac{h_\Omega^{2r}}{\tau} \left\| \frac{\partial c}{\partial t} \right\|_{L^2([t^{n-1}, t^n]; H^r(\Omega))}^2 + M \frac{h_\Lambda^4}{\tau} \left\| \frac{\partial \hat{c}}{\partial t} \right\|_{L^2(t^{n-1}, t^n; H^2(\Lambda))}^2 \\
&\quad + M h_\Omega^{2r-2} \|c(t^n)\|_{H^r(\Omega)}^2 + M h_\Lambda^2 \|\hat{c}(t^n)\|_{H^2(\Lambda)}^2. \tag{27}
\end{aligned}$$

The rest of the proof follows a standard technique. After dropping some positive terms in the left-hand side, we multiply (27) by 2τ , sum from $n = 1$ to $n = m$ for any $m \geq 1$, assume that $\tau \leq 1/2$ and apply Gronwall's lemma to obtain:

$$\begin{aligned} & \|e^m\|_{L^2(\Omega)}^2 + \|\mathcal{D}|^{1/2}\hat{e}^m\|_{L^2(\Lambda)}^2 + \frac{k_0}{2}\tau \sum_{n=1}^m \|\nabla e^n\|_{L^2(\Omega)}^2 + C_a\tau \sum_{n=1}^m |\hat{e}^n|_{\text{DG}}^2 \\ & \leq \|e^0\|_{L^2(\Omega)}^2 + \|\mathcal{D}|^{1/2}\hat{e}^0\|_{L^2(\Lambda)}^2 + M\tau^2 \left(\left\| \frac{\partial^2 c}{\partial t^2} \right\|_{L^2([0,T] \times \Omega)}^2 + \left\| \frac{\partial^2 \hat{c}}{\partial t^2} \right\|_{L^2([0,T] \times \Lambda)}^2 \right) \\ & \quad + Mh_\Omega^{2r-2} \left(\left\| \frac{\partial c}{\partial t} \right\|_{L^2(0,T;H^r(\Omega))}^2 + \|c\|_{L^2(0,T;H^r(\Omega))}^2 \right) \\ & \quad + Mh_\Lambda^2 \left(\left\| \frac{\partial \hat{c}}{\partial t} \right\|_{L^2(0,T;H^2(\Lambda))}^2 + \|\hat{c}\|_{L^2(0,T;H^2(\Lambda))}^2 \right). \end{aligned}$$

The final result is obtained by first using the approximation bounds (20) and (22) for the initial errors e^0 and \hat{e}^0 , and second by using triangle inequalities and optimal bounds for the approximation errors. \square

6 Numerical results

In this section, we present results for a manufactured solution for a domain with a vertical line and for an unknown solution for a domain with a diagonal line.

6.1 Manufactured solution

To test convergence, we consider a manufactured solution and compute error rates. The 3D domain is defined as the unit cube centered at the origin, $\Omega = (-0.5, 0.5)^3$. The 1D vessel is encompassed within Ω and is a vertical line $\Lambda = \{(0, 0, z), z \in (-0.5, 0.5)\}$. Our manufactured solution is similar to the ones used in [11, 13]. Using polar coordinates, $r = (x^2 + y^2)^{1/2}$, we have

$$\hat{c}(z, t) = t(\sin(\pi z) + 2), \quad c(x, y, z, t) = \begin{cases} \frac{1}{2}(1 + R \ln(\frac{r}{R}))\hat{c}(z, t), & r > R, \\ \frac{1}{2}\hat{c}(z, t), & r \leq R. \end{cases}$$

where R is the radius of cylinder with centerline Λ . We choose $R = 0.05$. The other parameters are: $\kappa = \hat{\kappa} = \gamma = \hat{U} = 1$. Since the 1D vessel is aligned with the z -axis, the primary direction of flow is in the vertical direction. To ensure advection in the 3D domain occurs in the same direction as the 1D domain, we define the 3D velocity as $\mathbf{U} = (0, 0, \hat{U})$. The prescribed concentration c^{in} is deduced from the exact solution \hat{c} . We implemented the numerical scheme using FEniCS and the (FEniCS)_{ii} module that contains the implementation of the lateral average operator [17–19]. For the DG parameters, we choose $\epsilon = 1$ and $\sigma = 50$. Simulations are ran for a time period of $T = 1.0$. Figure 1 shows the numerical solutions at $T = 1$ in the whole domain (left figure) and in the plane $z = 1/2$ (right figure). We perform a convergence study and compute the errors in the gradient norm and in the L^2 norm on successively refined uniform meshes. Table 1 and Table 2 display the errors and their corresponding rates for a mesh size $h_\Omega = h_\Lambda = 1/2^i$ for $2 \leq i \leq 6$, at the final time $T = 1$. The time

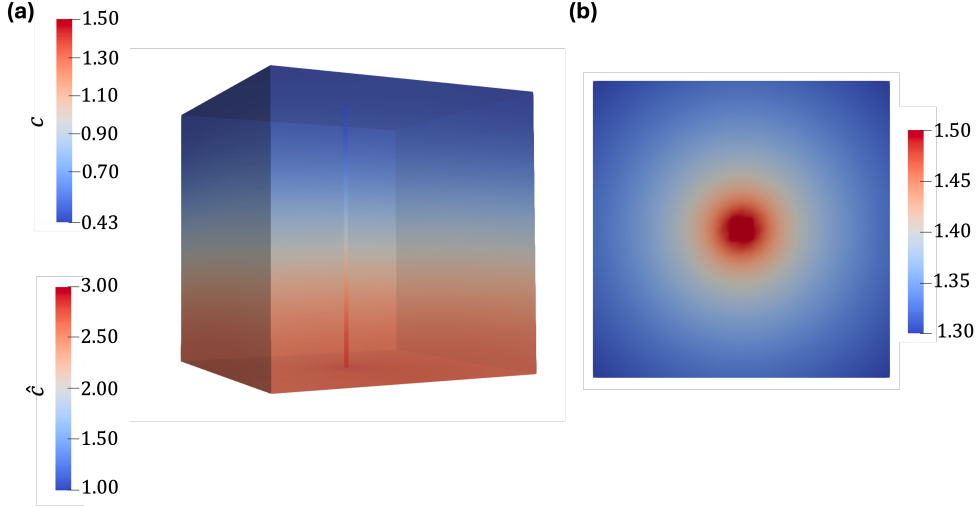


Fig. 1 Numerical prediction at $T = 1$ of the manufactured solution: left figure shows both concentrations in the whole domain and the right figure shows the concentrations in the plane $z = 1/2$.

Table 1 Numerical errors at $T = t^m = 1$ in the gradient norm and L^2 norm.

$h_\Omega = h_\Lambda$	$\ \nabla c(\cdot, T) - \nabla c_h^m\ _{L^2(\Omega)}$	Rate	$\ c(\cdot, T) - c_h^m\ _{L^2(\Omega)}$	Rate
1/4	2.5×10^{-1}		1.9×10^{-2}	
1/8	1.4×10^{-1}	0.82	5.4×10^{-3}	1.78
1/16	9.1×10^{-2}	0.63	1.7×10^{-3}	1.63
1/32	5.6×10^{-2}	0.71	5.2×10^{-4}	1.75
1/64	3.4×10^{-2}	0.73	1.4×10^{-4}	1.89

Table 2 Numerical errors at $T = t^m = 1$ in the broken gradient norm and L^2 norm.

$h_\Omega = h_\Lambda$	$\sum_{i=1}^N \ \nabla \hat{c}(\cdot, T) - \nabla \hat{c}_h^m\ _{L^2([s_{i-1}, s_i])}$	Rate	$\ \hat{c}(\cdot, T) - c_h^m\ _{L^2(\Lambda)}$	Rate
1/4	5.0×10^{-1}		4.1×10^{-2}	
1/8	2.5×10^{-1}	0.99	2.3×10^{-2}	0.82
1/16	1.3×10^{-1}	0.99	1.3×10^{-2}	0.81
1/32	6.3×10^{-2}	0.99	6.2×10^{-3}	1.07
1/64	3.1×10^{-2}	1.01	2.3×10^{-3}	1.43

step size is $\tau = 0.1h_\Omega$. We observe that the rates in the gradient norms approach the theoretical rate $1/2$ for the 3D solution and 1 for the 1D solution despite the coupling. The L^2 rates have not converged yet. Optimally they should approach $3/2$ for the 3D solution and 2 for the 1D solution but there is not theoretical proof of convergence in L^2 .

6.2 Diagonal line example

We also test convergence without a manufactured solution by defining a diagonal line of length L , within the 3D domain and comparing the results on a family of uniform meshes. We let the true solution be defined as the solution obtained with a fine mesh, $h_\Omega = h_\Lambda = h^* = 1/64$. Again, $\Omega = (-0.5, 0.5)^3$ and Λ is now the diagonal line encompassed within Ω :

$$\Lambda = \{(x, y, z), x \in (-0.4, 0.4), y \in (-0.4, 0.4), z \in (-0.4, 0.4)\}.$$

The final time is $T = 1$ and the time step is $\tau = 0.1h_\Omega$. The solute is injected at the inlet of the 1D line for 0.1s with $\hat{c}^{\text{in}} = 5$. The velocity fields are $\tilde{U} = 1$ and $\mathbf{U} = \frac{\tilde{U}}{\sqrt{3}}(1, 1, 1)$, which is the unit tangent vector along the diagonal line. We implement three different cases:

- Case 1: Constant radius $R = 0.05$ and constant $\gamma = 0.1$.
- Case 2: Constant $\gamma = 0.1$ and smooth varying radius,

$$R(s) = R_{\min} + \frac{R_{\max} - R_{\min}}{2} \left(1 + \tanh \left(\beta \left(\frac{s}{L} - \frac{1}{2} \right) \right) \right),$$

where $R_{\min} = 0.05$, $R_{\max} = 0.08$ are the minimum and maximum radii respectively, and $\beta = 8$.

- Case 3: Smooth varying radius as defined above and piecewise constant $\gamma(s)$,

$$\gamma(s) = \begin{cases} 0 & 0 \leq s < L/3, \\ 0.05 & L/3 \leq s < 2L/3, \\ 0.1 & 2L/3 \leq s \leq L. \end{cases}$$

From Figure 2, we see the expected behavior in the 3D tissue for all cases shown at different times: $t = 0.0125$, $t = 0.5$ and $t = 1$. In case 1 there is uniform exchange between the tissue and the vessel. In case 2 we have an increasing radius along the vessel length and we see the band of exchange increases likewise. In case 3, there is no exchange along the part of the vessel where $\gamma = 0$ and the solute begins to perfuse into Ω at $L/3$ where we have $\gamma = 0.05$. Figure 3 shows the expected behavior of the concentration within the vessel itself. Overall for all three cases, most of the solute has diffused into the surrounding tissue at the final time. Case 2 shows the least amount of solute left in the vessel whereas case 1 shows the most amount left (almost double the amount). This is due to the increase of 3D-1D exchange because of the larger radius value. There are differences between the three cases regarding the evolution of the concentration, which is shown on the figures at half-time. At time $t = 0.5$, case 3 shows the largest value of the concentration near the inlet, which is consistent with the fact that the first third of the vessel is impermeable with no exchange. These simulations show the impact of the value of the permeability and radius of the vessel.

Table 3 shows relative L^2 norms of errors for both domains across the three cases. In all cases the errors decrease monotonically as mesh refinement increases, indicating

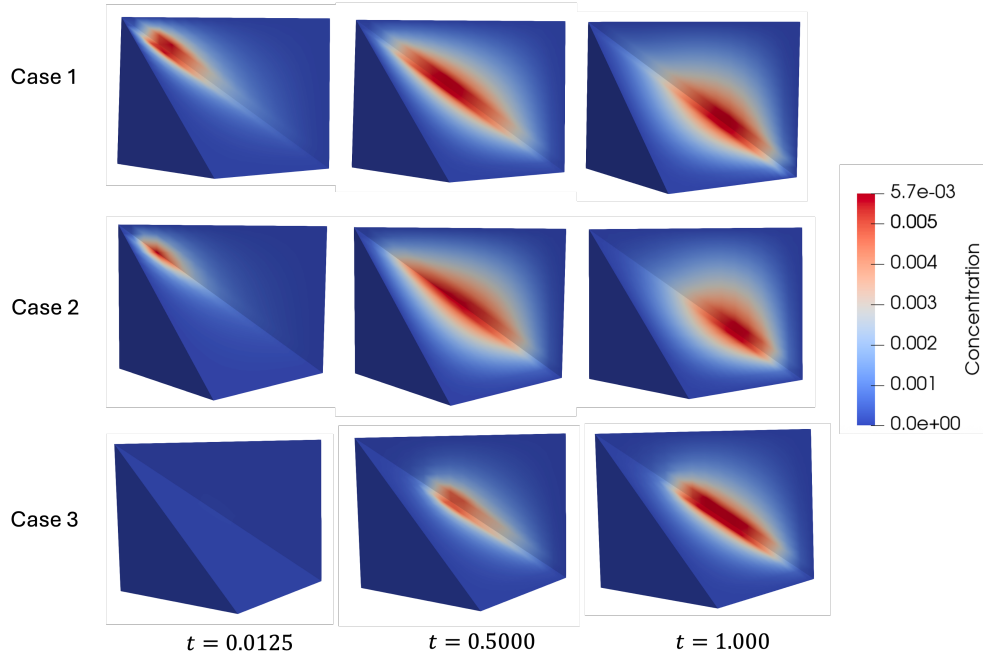


Fig. 2 Simulation results of a given concentration administered at the inlet of Λ , traveling to the outlet and diffusing into Ω over a time interval $[0, 1]$. Case 1: constant radius and global γ , Case 2: smooth varying radius and global γ , and Case 3: smooth varying radius and piecewise constant γ .

convergence. Although case 3 shows an accelerated convergence to the fine grid solution, the results indicate consistent error reduction across mesh refinement indicating stability and accuracy of the model.

Table 3 L^2 norms of errors between the numerical solutions obtained on a mesh of size $h_\Omega = h_\Lambda$ and a finer mesh of size $h^* = 1/64$.

	$h_\Omega = h_\Lambda$	$\ c_h^m - c_{h^*}^m\ _{L^2(\Omega)}$	Rate	$\ \hat{c}_h^m - \hat{c}_{h^*}^m\ _{L^2(\Lambda)}$	Rate
Case 1	1/4	5.2×10^{-1}		2.0×10^{-1}	
	1/8	2.2×10^{-1}	1.245	6.5×10^{-2}	1.628
	1/16	8.9×10^{-2}	1.306	1.7×10^{-2}	1.914
	1/32	2.5×10^{-2}	1.832	4.1×10^{-3}	2.092
Case 2	1/4	2.6×10^{-1}		3.7×10^{-1}	
	1/8	8.6×10^{-2}	1.61	9.0×10^{-2}	2.03
	1/16	1.6×10^{-2}	2.43	1.5×10^{-2}	2.56
	1/32	3.5×10^{-3}	2.16	3.1×10^{-3}	2.29
Case 3	1/4	1.3×10^{-1}		1.2×10^{-1}	
	1/8	2.5×10^{-2}	2.37	1.3×10^{-2}	3.19
	1/16	2.3×10^{-4}	6.82	9.0×10^{-6}	10.50
	1/32	2.4×10^{-6}	6.58	4.7×10^{-10}	14.23

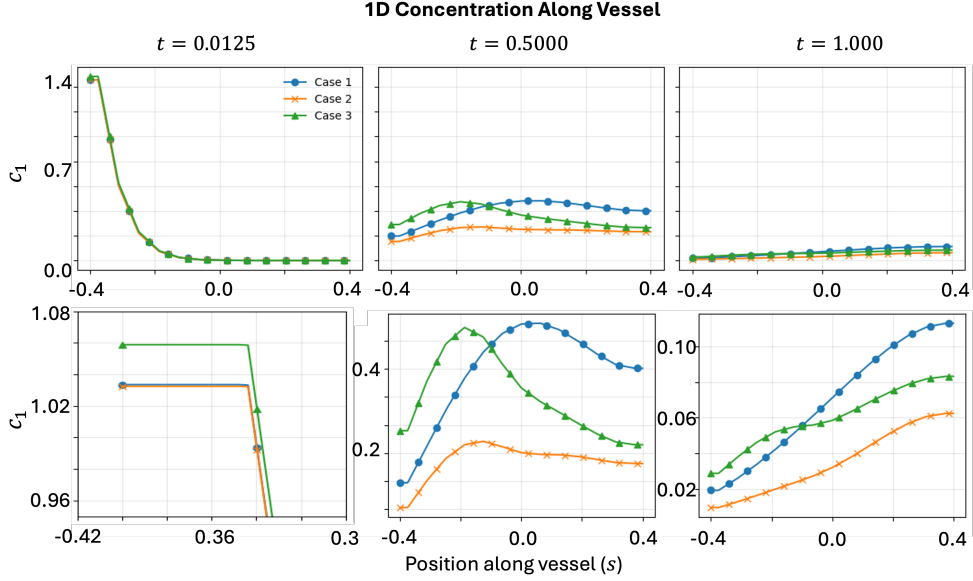


Fig. 3 Concentrations c_1 plotted along the diagonal vessel defined in Section 6.2 at times 0.0125, 0.005 and 1. The top rows shows concentrations at each time in the same scale, while the bottom row has a varying scale to highlight the differences between cases.

7 Conclusion

A numerical scheme is analyzed for the coupled 3D-1D transport problem. The concentration in the 3D domain is approximated by continuous piecewise polynomials and the concentration in the 1D domain is approximated by discontinuous polynomials. Error bounds that combine both 3D and 1D errors in L^2 in time and gradient in space are optimal with respect to the time step and the regularity of the weak solution. In addition, bounds of the errors in $L^\infty(L^2)$ are also derived.

Because of the use of finite elements for the 3D problem, the velocity field is assumed to be either divergence free or to be bounded by the diffusion coefficient in the 3D domain. In order to remove these assumptions, the 3D transport problem should be discretized by a discontinuous Galerkin method. The lack of consistency for the DG method in the 3D domain is a challenge. This will be the object of future work.

Acknowledgements. The authors acknowledge partial funding from NSF-DMS 2513092, NSF-DMS 2231482, and NIH 1R01CA301555-01.

Declarations

- Funding: The authors acknowledge partial funding from NSF-DMS 2513092, NSF-DMS 2231482, NIH 1L40HL181846-01, and NIH 1R01CA301555-01.
- Competing Interests: The authors have no competing interests to declare that are relevant to the content of this article.

- Ethics approval and consent to participate: Not applicable
- Consent for publication: Not applicable
- Data availability: Not applicable
- Materials availability: Not applicable
- Code availability: Not applicable
- Author contribution: Not applicable

Appendix A Derivation of the numerical scheme

We consider first the time discretization of (1)-(2) and obtain at time t^n the semi-discrete equations:

$$\begin{aligned} \frac{c^n - c^{n-1}}{\tau} - \nabla \cdot (\kappa \nabla c^n) + \nabla \cdot (\mathbf{U} c^n) + \gamma(\bar{c}^n - \hat{c}^n) \delta_\Lambda &= f(t^n), \text{ in } \Omega, \\ |\mathcal{D}(s)| \frac{\hat{c}^n - \hat{c}^{n-1}}{\tau} - \frac{\partial}{\partial s} \left(|\mathcal{D}(s)| \hat{\kappa} \frac{\partial \hat{c}^n}{\partial s} \right) + \frac{\partial}{\partial s} \left(|\mathcal{D}(s)| \hat{U} \hat{c}^n \right) + |\partial \mathcal{D}(s)| \gamma (\hat{c}^n - \bar{c}^n) &= \hat{f}(t^n), \text{ in } \Lambda. \end{aligned}$$

After, we spatially discretize the first equation above by the finite element method, we multiply it by a test function v_h and integrate over Ω .

$$\int_{\Omega} \frac{c_h^n - c_h^{n-1}}{\tau} v_h + \int_{\Omega} \kappa \nabla c_h^n \cdot \nabla v_h - \int_{\Omega} \mathbf{U} c_h^n \cdot \nabla v_h + \int_{\Lambda} \gamma |\partial \mathcal{D}| (c_h^n - \hat{c}_h^n) \bar{v}_h = \int_{\Omega} f(\cdot, t^n) v_h.$$

For the second equation, we apply the interior penalty discontinuous Galerkin method for spatial discretizations. For notational convenience, $\partial_s \hat{v}$ denotes the partial derivative of any function \hat{v} with respect to s . Then, we multiply the equation by a test function \hat{v}_h , integrate by parts over one interval $[s_{i-1}, s_i]$ and sum over all intervals.

$$\begin{aligned} \int_{\Lambda} |\mathcal{D}| \frac{\hat{c}_h^n - \hat{c}_h^{n-1}}{\tau} \hat{v}_h + \sum_{i=1}^N \int_{s_{i-1}}^{s_i} |\mathcal{D}| \hat{\kappa} \partial_s \hat{c}_h^n \partial_s \hat{v}_h - \sum_{i=1}^{N-1} [|\mathcal{D}| \hat{\kappa} \partial_s \hat{c}_h^n \hat{v}_h]_{s_i} \\ + (|\mathcal{D}| \hat{\kappa} \partial_s \hat{c}_h^n \hat{v}_h) \Big|_{s_0} - (|\mathcal{D}| \hat{\kappa} \partial_s \hat{c}_h^n \hat{v}_h) \Big|_{s_N} - \sum_{i=1}^N \int_{s_{i-1}}^{s_i} \hat{U} |\mathcal{D}| \hat{c}_h^n \partial_s \hat{v}_h + \sum_{i=1}^{N-1} \hat{U} [\hat{c}_h^n |\mathcal{D}| \hat{v}_h]_{s_i} \\ + \hat{U} (|\mathcal{D}| \hat{c}_h^n \hat{v}_h) \Big|_{s_N} - \hat{U} (|\mathcal{D}| \hat{c}_h^n \hat{v}_h) \Big|_{s_0} + \int_{\Lambda} \gamma |\partial \mathcal{D}| (\hat{c}_h^n - \bar{c}_h^n) \hat{v}_h = \int_{\Lambda} \hat{f}(\cdot, t^n) \hat{v}_h. \end{aligned}$$

Observe that for $1 \leq i \leq N-1$, since the exact solution belongs to $H^2(\Lambda)$

$$[|\mathcal{D}| \hat{\kappa} \partial_s \hat{c}_h^n \hat{v}_h]_{s_i} = \{|\mathcal{D}| \hat{\kappa} \partial_s \hat{c}_h^n\}_{s_i} [\hat{v}_h]_{s_i}, \quad [\hat{c}_h^n |\mathcal{D}| \hat{v}_h]_{s_i} = |\mathcal{D}(s_i)| \hat{c}_h^n(s_i^-) [\hat{v}_h]_{s_i}. \quad (\text{A1})$$

Using the boundary conditions (5), (6), we rewrite the equation above as:

$$\int_{\Lambda} |\mathcal{D}| \frac{\hat{c}_h^n - \hat{c}_h^{n-1}}{\tau} \hat{v}_h + \sum_{i=1}^N \int_{s_{i-1}}^{s_i} |\mathcal{D}| \hat{\kappa} \partial_s \hat{c}_h^n \partial_s \hat{v}_h - \sum_{i=1}^{N-1} \{|\mathcal{D}| \hat{\kappa} \partial_s \hat{c}_h^n\}_{s_i} [\hat{v}_h]_{s_i}$$

$$\begin{aligned}
& - \sum_{i=1}^N \int_{s_{i-1}}^{s_i} \hat{U} |\mathcal{D}| \hat{c}_h^n \partial_s \hat{v}_h + \sum_{i=1}^{N-1} \hat{U} |\mathcal{D}(s_i)| \hat{c}_h^n(s_i^-) [\hat{v}_h]_{s_i} \\
& + \hat{U} |\mathcal{D}(L)| \hat{c}_h^n(L) \hat{v}_h(L) + \int_{\Lambda} \gamma |\partial \mathcal{D}| (\hat{c}_h^n - \bar{c}_h^n) \hat{v}_h = |\mathcal{D}(0)| \hat{U} c_h^{\text{in}} v_h(0) + \int_{\Lambda} \hat{f}(\cdot, t^n) \hat{v}_h.
\end{aligned}$$

To conclude we add to the left-hand side of the equation the symmetrization and penalty terms, that vanish for the exact solution.

Appendix B Proof of coercivity (13)

This proof follows exactly the one given in Section 2.7 of [16] and uses the following trace inequality. There is a positive constant C_t such that

$$\forall \hat{v} \in \mathbb{P}_k([s_{i-1}, s_i]), \quad \left| \frac{\partial \hat{v}}{\partial s}(s) \right| \leq C_t h_i^{-1/2} \left\| \frac{\partial \hat{v}}{\partial s} \right\|_{L^2([s_{i-1}, s_i])}, \quad s = s_i, s_{i-1}, \quad (\text{B2})$$

where $h_i = s_i - s_{i-1}$. Using the trace inequality above and Cauchy-Schwarz's inequality, we obtain:

$$\left\{ |D(s)| \frac{\partial \hat{v}}{\partial s} \right\}_{s_i} [\hat{v}]_{s_i} \leq \left(\frac{C_t d_1}{2h_i^{1/2}} \left\| \frac{\partial \hat{v}}{\partial s} \right\|_{L^2([s_{i-1}, s_i])} + \frac{C_t d_1}{2h_{i+1}^{1/2}} \left\| \frac{\partial \hat{v}}{\partial s} \right\|_{L^2([s_i, s_{i+1}])} \right) \left(\frac{1}{h_{\Lambda}} \right)^{\frac{1}{2} - \frac{1}{2}} [\hat{v}]_{s_i}.$$

By summing over i , using Cauchy-Schwarz's inequality and Young's inequality (with $\delta > 0$), we obtain:

$$\begin{aligned}
\sum_{i=1}^{N-1} \left\{ |D(s)| \frac{\partial \hat{v}}{\partial s} \right\}_{s_i} [\hat{v}]_{s_i} & \leq C_t d_1 \sqrt{2} \left(\sum_{i=1}^{N-1} \frac{1}{h_{\Lambda}} [\hat{v}]_{s_i}^2 \right)^{1/2} \left(\sum_{i=1}^N \left\| \frac{\partial \hat{v}}{\partial s} \right\|_{L^2([s_{i-1}, s_i])}^2 \right)^{1/2} \\
& \leq \frac{\delta}{2} \sum_{i=1}^N \left\| |D|^{1/2} \frac{\partial \hat{v}}{\partial s} \right\|_{L^2([s_{i-1}, s_i])}^2 + \frac{C_t^2 d_1^2}{\delta d_0} \sum_{i=1}^{N-1} \frac{1}{h_{\Lambda}} [\hat{v}]_{s_i}^2.
\end{aligned}$$

Using the above inequality we obtain a lower bound for a_{Λ} :

$$a_{\Lambda}(\hat{v}, \hat{v}) \geq \left(1 - \frac{\delta}{2}(1 + \epsilon) \right) \sum_{i=1}^N \left\| |D|^{1/2} \frac{\partial \hat{v}}{\partial s} \right\|_{L^2([s_{i-1}, s_i])}^2 + \sum_{i=1}^{N-1} \frac{\sigma - \frac{C_t^2 d_1^2}{\delta d_0} (1 + \epsilon)}{h_{\Lambda}} [\hat{v}]_{s_i}^2.$$

If $\epsilon = 1$ or 0 , we choose $\delta = \frac{1}{2}$ and $\sigma \geq \frac{4C_t^2 d_1^2}{d_0}$, thus we have the coercivity result with $C_a = 1/2$. The result is trivially correct if $\epsilon = -1$.

Appendix C Proof of positivity (14)

We write

$$b_\Lambda(\hat{v}, \hat{v}) = - \sum_{i=1}^N \int_{s_{i-1}}^{s_i} |\mathcal{D}| \hat{U} \hat{v} \frac{\partial \hat{v}}{\partial s} + \sum_{i=1}^{N-1} |\mathcal{D}(s_i)| \hat{U} \hat{v}(s_i^-) [\hat{v}]_{s_i} + |\mathcal{D}(L)| \hat{U} (\hat{v}(L))^2.$$

Since \hat{U} is a constant, we write

$$- \int_{s_{i-1}}^{s_i} |\mathcal{D}| \hat{U} \hat{v} \frac{\partial \hat{v}}{\partial s} = \frac{1}{2} \hat{U} \int_{s_{i-1}}^{s_i} \frac{d|\mathcal{D}|}{ds} \hat{v}^2 + \frac{1}{2} \hat{U} (|\mathcal{D}(s_{i-1}^+)| \hat{v}^2(s_{i-1}^+) - |\mathcal{D}(s_i^-)| \hat{v}^2(s_i^-)).$$

We thus obtain since $|\mathcal{D}|$ is continuous and $d(|\mathcal{D}|)/ds \geq 0$

$$\begin{aligned} b_\Lambda(\hat{v}, \hat{v}) &\geq - \sum_{i=1}^{N-1} \frac{1}{2} \hat{U} |\mathcal{D}(s_i)| [\hat{v}^2]_{s_i} + \frac{1}{2} |\mathcal{D}(0)| \hat{U} (\hat{v}(0))^2 \\ &\quad + \frac{1}{2} |\mathcal{D}(L)| \hat{U} (\hat{v}(L))^2 + \sum_{i=1}^{N-1} \hat{U} |\mathcal{D}(s_i)| \hat{v}|_{s_i^-} [\hat{v}]_{s_i} \\ &\geq \frac{1}{2} \sum_{i=1}^{N-1} \hat{U} |\mathcal{D}(s_i)| ([\hat{v}]_{s_i})^2 + \frac{1}{2} |\mathcal{D}(0)| \hat{U} (\hat{v}(0))^2 + \frac{1}{2} |\mathcal{D}(L)| \hat{U} (\hat{v}(L))^2. \end{aligned}$$

Appendix D Bound for term T_5

We want to prove

$$T_5 \leq \frac{\epsilon_5}{2} |\hat{e}^n|_{\text{DG}}^2 + \frac{1}{2\epsilon_5} M h_\Lambda^2 \|\hat{c}(t^n)\|_{H^2(\Lambda)}^2.$$

We expand the term T_5 :

$$\begin{aligned} a_\Lambda(\hat{\xi}(t^n), \hat{e}^n) &= \sum_{i=1}^N \int_{s_{i-1}}^{s_i} |D(s)| \frac{\partial \hat{\xi}(t^n)}{\partial s} \frac{\partial \hat{e}^n}{\partial s} - \sum_{i=1}^{N-1} \left\{ |D(s)| \frac{\partial \hat{\xi}(t^n)}{\partial s} \right\}_{s_i} [\hat{e}^n]_{s_i} \\ &\quad - \epsilon \sum_{i=1}^{N-1} \left\{ |D(s)| \frac{\partial \hat{e}^n}{\partial s} \right\}_{s_i} [\hat{\xi}(t^n)]_{s_i} + \sum_{i=1}^{N-1} \frac{\sigma}{h_\Lambda} [\hat{\xi}(t^n)]_{s_i} [\hat{e}^n]_{s_i}. \end{aligned}$$

Using the Cauchy-Schwarz's inequality, Young's inequality and approximation property (24), we have:

$$\left| \sum_{i=1}^N \int_{s_{i-1}}^{s_i} |D(s)| \frac{\partial \hat{\xi}(t^n)}{\partial s} \frac{\partial \hat{e}^n}{\partial s} \right| \leq \frac{\epsilon_5}{4} \sum_{i=1}^N \left\| |D|^{\frac{1}{2}} d_s \hat{e}^n(s) \right\|_{L^2([s_{i-1}, s_i])}^2$$

$$\begin{aligned}
& + \frac{1}{\epsilon_5} \sum_{i=1}^N \left\| |D|^{\frac{1}{2}} \frac{\partial \hat{\xi}(t^n)}{\partial s} \right\|_{L^2([s_{i-1}, s_i])}^2 \\
& \leq \frac{\epsilon_5}{4} |\hat{e}^n|_{\text{DG}}^2 + \frac{M}{\epsilon_5} h_\Lambda^2 \|\hat{c}(t^n)\|_{H^2(\Lambda)}^2.
\end{aligned}$$

For the second term, using triangle inequality, Young's inequality, trace inequality and approximation properties (24), we obtain:

$$\begin{aligned}
\left| - \sum_{i=1}^{N-1} \left\{ |D(s)| \frac{\partial \hat{\xi}(t^n)}{\partial s} \right\}_{s_i} [\hat{e}^n]_{s_i} \right| & \leq \frac{\epsilon_5}{4} \sum_{i=1}^{N-1} \frac{\sigma}{h_\Lambda} [\hat{e}^n]_{s_i}^2 \\
& + \sum_{i=1}^{N-1} \frac{d_1^2 h_\Lambda}{4\sigma \epsilon_5} \left(\left| \frac{\partial \hat{\xi}(t^n)}{\partial s}(s_{i-1}^+) \right|^2 + \left| \frac{\partial \hat{\xi}(t^n)}{\partial s}(s_i^-) \right|^2 \right) \\
& \leq \frac{\epsilon_5}{4} |\hat{e}^n|_{\text{DG}}^2 + \frac{M}{\epsilon_5} h_\Lambda^2 \|\hat{c}(t^n)\|_{H^2(\Lambda)}^2.
\end{aligned}$$

Similarly, we have for the third term with the trace inequality (B2), Cauchy-Schwarz's and Young's inequalities and (22), (24):

$$\begin{aligned}
\left| \sum_{i=1}^{N-1} \left\{ |D(s)| \frac{\partial \hat{e}^n}{\partial s} \right\}_{s_i} [\hat{\xi}(t^n)]_{s_i} \right| & \leq \sum_{i=1}^{N-1} \|[\hat{\xi}(t^n)]_{s_i}\| C_t \frac{d_1}{2h_\Lambda^{1/2}} \left(\left\| \frac{\partial \hat{e}^n}{\partial s} \right\|_{L^2([s_{i-1}, s_i])} + \left\| \frac{\partial \hat{e}^n}{\partial s} \right\|_{L^2([s_i, s_{i+1}])} \right) \\
& \leq \frac{\epsilon_5}{4} |\hat{e}^n|_{\text{DG}}^2 + \frac{M}{\epsilon_5} h_\Lambda^3 \|\hat{c}\|_{H^2(\Lambda)}^2.
\end{aligned}$$

For the last term, we use (22) and (24):

$$\begin{aligned}
\left| \sum_{i=1}^{N-1} \frac{\sigma}{h_\Lambda} [\hat{\xi}(t^n)]_{s_i} [\hat{e}^n]_{s_i} \right| & \leq \frac{\epsilon_5}{4} \sum_{i=1}^{N-1} \frac{\sigma}{h_\Lambda} [\hat{e}^n]_{s_i}^2 + \frac{1}{\epsilon_5} \sum_{i=1}^{N-1} \frac{\sigma}{h_\Lambda} [\hat{\xi}(t^n)]_{s_i}^2 \\
& \leq \frac{\epsilon_5}{4} |\hat{e}^n|_{\text{DG}}^2 + M h_\Lambda^2 \|\hat{c}\|_{H^2(\Lambda)}^2.
\end{aligned}$$

By summing each term above, we obtain the desired bound for T_5 .

References

- [1] Cattaneo, L., Zunino, P.: A computational model of drug delivery through microcirculation to compare different tumor treatments. *International Journal for Numerical Methods in Biomedical Engineering* **30**(11), 1347–1371 (2014)
- [2] Notaro, D., Cattaneo, L., Formaggia, L., Scotti, A., Element, P.Z.A.M.F.: Method for Modeling the Fluid Exchange Between Microcirculation and Tissue Interstitium. *Advances in Discretization Methods*. Springer (2016)

- [3] Köppl, T., Vidotto, E., Wohlmuth, B.: A 3D-1D coupled blood flow and oxygen transport model to generate microvascular networks. *International Journal for Numerical Methods in Biomedical Engineering* **36**(10), 3386 (2020)
- [4] Fritz, M., Köppl, T., Oden, J.T., Wagner, A., Wohlmuth, B., Wu, C.: A 1D–0D–3D coupled model for simulating blood flow and transport processes in breast tissue. *International Journal for Numerical Methods in Biomedical Engineering* **38**(7), 3612 (2022)
- [5] Gjerde, I.G., Kumar, K., Nordbotten, J.M.: A singularity removal method for coupled 1D–3D flow models. *Computational Geosciences* **24**(2), 443–457 (2020)
- [6] Malenica, L., Gotovac, H., Kamber, G., Simunovic, S., Allu, S., Divic, V.: Groundwater flow modeling in karst aquifers: Coupling 3D matrix and 1D conduit flow via control volume isogeometric analysis—experimental verification with a 3D physical model. *Water* **10**(12), 1787 (2018)
- [7] Cerroni, D., Laurino, F., Zunino, P.: Mathematical analysis, finite element approximation and numerical solvers for the interaction of 3D reservoirs with 1D wells. *GEM-International Journal on Geomathematics* **10**(1), 4 (2019)
- [8] Gjerde, I., Kumar, K., Nordbotten, J.: Well modelling by means of coupled 1D-3D flow models. In: *ECMOR XVI-16th European Conference on the Mathematics of Oil Recovery*, vol. 2018, pp. 1–12 (2018). European Association of Geoscientists & Engineers
- [9] Llau, A., Jason, L., Dufour, F., Baroth, J.: Finite element modelling of 1d steel components in reinforced and prestressed concrete structures. *Engineering Structures* **127**, 769–783 (2016)
- [10] D’Angelo, C., Quarteroni, A.M.: On the coupling of 1D and 3D diffusion-reaction equations. applications to tissue perfusion problems. *Mathematical Models and Methods in Applied Sciences* **18**, 1481–1505 (2008)
- [11] Laurino, F., Zunino, P.: Derivation and analysis of coupled PDEs on manifolds with high dimensionality gap arising from topological model reduction. *ESAIM Mathematical Modelling and Numerical Analysis* **53**, 2047–2080 (2019)
- [12] Masri, R., Zeinhofer, M., Kuchta, M., Rognes, M.E.: The modelling error in multi-dimensional time-dependent solute transport models. *ESAIM: Mathematical Modelling and Numerical Analysis* **58**(5), 1681–1724 (2024)
- [13] Masri, R., Kuchta, M., Riviere, B.: Discontinuous Galerkin methods for 3D-1D systems. *SIAM Journal on Numerical Analysis* **62**(4), 1814–1843 (2024)
- [14] Scott, L.R., Zhang, S.: Finite element interpolation of nonsmooth functions satisfying boundary conditions. *Mathematics of Computation* **54**(190), 483–493

(1990)

- [15] Bernardi, C., Girault, V., Raviart, P.A., Riviere, B.: *Mathematics and Finite Element Discretizations of Incompressible Navier–Stokes Flows: Revised and Expanded Edition*. Society for Industrial and Applied Mathematics (2024)
- [16] Riviere, B.: *Discontinuous Galerkin Methods for Solving Elliptic and Parabolic Equations: Theory and Implementation*. Society for Industrial and Applied Mathematics (SIAM, 3600 Market Street, Floor 6, Philadelphia, PA 19104) (2008)
- [17] Logg, A., Mardal, K.-A., Wells, G.: *Automated solution of differential equations by the finite element method: The FEniCS book*. Springer (2012)
- [18] Alnæs, M., Blechta, J., Hake, J., Johansson, A., Kehlet, B., Logg, A., Richardson, C., Ring, J., Rognes, M.E., Wells, G.N.: The FEniCS project version 1.5. *Archive of Numerical Software* **3**(100) (2015)
- [19] Kuchta, M.: Assembly of multiscale linear PDE operators. In: *Numerical Mathematics and Advanced Applications ENUMATH 2019: European Conference, Egmond Aan Zee, The Netherlands, September 30-October 4*, pp. 641–650 (2020). Springer